Simulations of acoustic scattering in duct systems with flow

A. Kierkegaard (1), S. Boij (1), G. Efraimsson (2)

(1) MWL, KTH, Stockholm, Sweden
(2) Linné FLOW Centre, KTH, Stockholm, Sweden

ABSTRACT

We present an efficient methodology to perform calculations of acoustic propagation and scattering by geometrical objects in ducts with flows. In this paper a methodology with a linearized Navier-Stokes equations solver in frequency domain is evaluated on a two-dimensional geometry of an in-duct area expansion. The Navier-Stokes equations are linearized around a time- independent mean flow that is obtained from an incompressible Reynolds Averaged Navier-Stokes solver which uses a k-ε turbulence model. A plane wave decomposition method based on acoustic pressure and velocity is used to extract the up- and downstream propagating waves. The scattering of the acoustic waves by the induct area expansion is calculated and compared to experiments. Frequencies in the plane wave range up to the cut-on frequency of the first higher order propagating acoustical mode are considered. The acoustical properties of the area expansion is presented in a scattering matrix form that can be used in acoustical two-port calculations on complex duct systems such as exhaust system mufflers and ventilation systems.

INTRODUCTION

Traffic is a major source of environmental noise in modern day society. The major noise sources on common road vehicles are engine noise, transmission noise, tire noise and, at high speeds, wind noise. At low speeds (<30-50 km/h), intake and exhaust noise are particularly important during acceleration. Subsequently, development of new vehicles is subject to increasingly firmer governmental legislations. One common way to reduce exhaust noise is to attach mufflers to the exhaust pipes. However, to develop prototypes of mufflers for evaluation is a costly and time-consuming process. As a consequence, in recent years so-called virtual prototyping has emerged as an alternative. Current industrial simulation methodologies are often rather crude, either neglecting mean flows or including only one-dimensional mean flows. Hence, improved, but still efficient, methods are needed to fully benefit from the possibilities of virtual prototyping.

Outside the acoustic source regions, the acoustic quantities are often small in comparison to the flow field quantities. In many cases it can be assumed that the flow field affects the sound waves, whereas the sound waves do not significantly affect the flow field. These types of cases enable a two-stage treatment of the acoustic wave propagation: firstly the mean flow can be calculated without considering any acoustic waves, and secondly the sound waves can be calculated with the flow field as input. In addition, the perturbations are often small enough to justify linearization. In such cases, a frequency domain approach can be taken.

However, it should be pointed out that this two-stage treatment is not always applicable. At certain conditions the acoustic field actually does couple with the mean flow field, and small changes in the acoustic field can disturb and alter the mean flow field, which in turn affect the acoustic field. In these cases a full treatment of the fluid dynamic equations are needed. A typical example of such a case is whistling tones generated in pipes. This paper describes the derivation and evaluation of a method to simulate sound propagation in two-dimensional confined geometries with arbitrary internal mean flows. A frequency domain linearized Navier-Stokes equations methodology is developed for acoustic wave propagation applications. The method is validated on a case of an in-duct area expansion.

Since most research efforts have been aimed at jet noise generation, where unsteady simulations are needed, few studies have paid attention to the possibilities of frequency-domain aeroacoustics. Examples are [1–3] where the Linearized Euler Equations and the Linearized Lilley's equation have been used. Other internal aeroacoustic simulations on geometries relevant to the work presented here, but performed with other methodologies can be found in, for example, [4–6]. The work presented in this paper aims as a step in the development of a simulation methodology for linear internal aeroacoustics.

THE LINEARIZED NAVIER-STOKES EQUATIONS

When studying propagation of aeroacoustic waves in flows where dissipative effects are taken into account, the viscous terms in the Navier-Stokes equations may not be neglected. In this section we derive a frequency domain formulation of the Navier-Stokes equations in which the viscous terms have been retained.

The full compressible Navier-Stokes equations have been chosen as a starting point. These can be written in dimensional form as, [7]:

$$\textbf{Continuity}: \quad \frac{D\rho}{Dt} + \rho \frac{\partial u_k}{\partial x_k} = 0$$

$$\textbf{Momentum}: \quad \rho \frac{Du_i}{Dt} = -\frac{\partial p}{\partial x_i} + \frac{\partial \tau_{ij}}{\partial x_j} + \rho F_i$$

$$\textbf{Energy}: \quad \rho \frac{De}{Dt} = -p\frac{\partial u_k}{\partial x_k} + \Phi + \frac{\partial}{\partial x_k}\left(\kappa \frac{\partial T}{\partial x_k}\right)$$
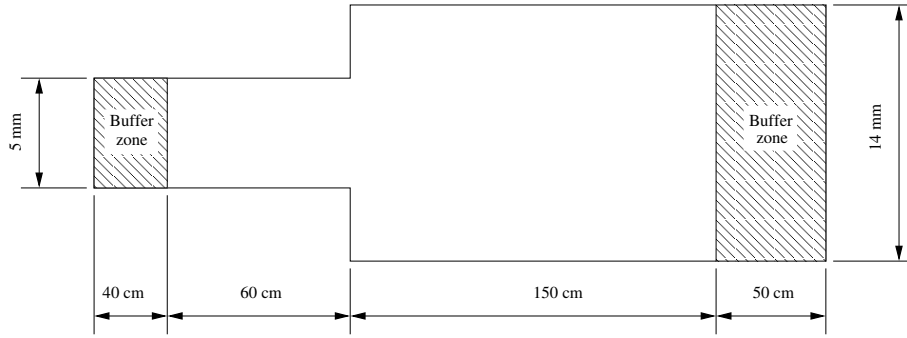
$$(1)$$

Figure 1: Schematic sketch of the geometry of the area expansion.

with

$$\Phi = \tau_{ij}\frac{\partial u_i}{\partial x_j}, \quad \tau_{ij} = \mu\left(\frac{\partial u_i}{\partial x_j}+\frac{\partial u_j}{\partial x_i}-\frac{2}{3}\frac{\partial u_k}{\partial x_k}\delta_{ij}\right) \quad (2)$$

and $e = e(p,T)$, $p = \rho RT$, where ρ is the density, p is the pressure, R is the universal gas constant, T is the absolute temperature, u_i is the velocity component in the i:th direction, τ_{ij} is the viscous stress tensor, F_i is a volume force in the i:th direction, e is the internal energy, κ is the thermal conductivity, μ is the dynamic viscosity, Φ is the dissipation function, D/Dt is the convective derivative, δ_{ij} is the Kronecker delta function, and the Einstein summation convention is used.

We first assume that the solution can be written as a sum of a time-independent meanflow term and a time-dependent perturbation term. For a 2D approximation this yields:

$$\begin{aligned}
\rho(\mathbf{x},t) = \rho_0(\mathbf{x})+\rho'(\mathbf{x},t), \qquad & u(\mathbf{x},t) = u_0(\mathbf{x})+u'(\mathbf{x},t),\\
v(\mathbf{x},t) = v_0(\mathbf{x})+v'(\mathbf{x},t), \qquad & p(\mathbf{x},t) = p_0(\mathbf{x})+p'(\mathbf{x},t)
\end{aligned}$$
$$(3)$$

where $u = u_1$ and $v = u_2$, are the perturbation velocities in horizontal and vertical directions, respectively. We then introduce Eqs. (3) in Eqs. (1) and assume that second order perturbation terms are sufficiently small to be neglected.

For simplicity we assume that the relation between pressure and density can be regarded as isentropic. This is an assumption, but is believed to make little difference [8], and is introduced to decrease the implementational and computational effort. In this case the pressure and density perturbations are related as where $c^2 = \gamma p_0/\rho_0$ is the square of the local adiabatic speed of sound, γ is the ratio of specific heats and p_0 and ρ_0 are the pressure and density of the mean flow, respectively [9]. With this relation, the energy equation is disconnected from the Navier-Stokes system of equations, and the size of the computational problem is reduced considerably.

For 2D geometries we arrive at the following formulation of the Linearized Navier-Stokes equations, as:

$\hat{\rho}$:

$$(u_0\ \ v_0)\nabla\hat{\rho}+\left(\frac{\partial u_0}{\partial x}+\frac{\partial v_0}{\partial y}-i\omega\right)\hat{\rho} = -\left(\frac{\partial\rho_0\hat{u}}{\partial x}+\frac{\partial\rho_0\hat{v}}{\partial y}\right)$$
$$(4)$$

$\hat{u}$:

$$\nabla^T\left(-\begin{pmatrix}\frac{4}{3}\mu & 0\\ 0 & \mu\end{pmatrix}\nabla\hat{u}\right)+\rho_0(u_0\ \ v_0)\nabla\hat{u}+\rho_0\left(\frac{\partial u_0}{\partial x}-i\omega\right)\hat{u} =$$

$$= \rho_0\hat{F}_x-\left(u_0\frac{\partial u_0}{\partial x}+v_0\frac{\partial u_0}{\partial y}\right)\hat{\rho}-c^2\frac{\partial\hat{\rho}}{\partial x}+\frac{1}{3}\mu\frac{\partial^2\hat{v}}{\partial x\partial y}-\rho_0\frac{\partial u_0}{\partial y}\hat{v}$$
$$(5)$$

$\hat{v}$:

$$\nabla^T\left(-\begin{pmatrix}\mu & 0\\ 0 & \frac{4}{3}\mu\end{pmatrix}\nabla\hat{v}\right)+\rho_0(u_0\ \ v_0)\nabla\hat{v}+\hat{\rho}_0\left(\frac{\partial v_0}{\partial y}-i\omega\right)\hat{v} =$$

$$= -c^2\frac{\partial\hat{\rho}}{\partial y}-\left(u_0\frac{\partial v_0}{\partial x}+v_0\frac{\partial v_0}{\partial y}\right)\hat{\rho}-\rho_0\frac{\partial v_0}{\partial x}\hat{u}+\frac{1}{3}\mu\frac{\partial^2\hat{u}}{\partial x\partial y}$$
$$(6)$$

where $\hat{\rho}$, $\hat{u}$ and $\hat{v}$ are the unknowns which represent the perturbations of the density and velocities in horizontal and vertical directions, respectively. Here u_0 and v_0 are the horizontal and vertical velocities of the mean flow, respectively. Also, i is the imaginary unit $i^2 = -1$, ω is the angular frequency, μ is the dynamic viscosity of the fluid, $\hat{F}$ is an externally applied volume force field used to introduce acoustic waves into the system, and $\nabla = (\partial/\partial x\ \ \partial/\partial y)^T$.

This is the form of the linearized Navier-Stokes equations that is used throughout the work in this paper.

THE AREA EXPANSION

The test geometry and flow case was chosen to correspond to the measurements of [10], which in addition has been analyzed theoretically in [8, 11].

A sketch of the geometry is shown in Figure 1. The height of the inlet duct was H = 5 cm, and the area expansion ratio 0.346, which yields a duct height of approximately 14 cm at the expanded side. Due to computational limits, only a small fraction of the total length of the duct system used in the experiment was possible to simulate. The geometry in the experiments was cylindrical axisymmetric, here however, as well as in the theoretical model, a rectangular 2D approximation is made.

MEAN FLOW

The mean flow was calculated with a steady-state incompressible $k-\varepsilon$ RANS model in Fluent. A turbulent inlet flow velocity profile was imposed at the left side of the duct system. The average flow velocity was set to match that of the experiments [10], which were performed at a Mach number of 0.08. This corresponds to a Reynolds number of about $9\cdot 10^4$ based on the duct height and mean flow velocity at the inlet.

The inlet duct length of the mean flow simulation was extended to 4 m, such that the velocity profile was stabilized at approximately x = -1, before reaching the start of the acoustical computational domain in Figure 1. An ambient pressure outflow boundary condition was imposed at the right boundary. Wall functions at $y+ \approx 1$ where used at the duct walls. The inlet turbulent length scale was set to 3.5 mm, and the turbulent intensity to 10%.

The mesh is structured and rectangular, and consists of 247120 nodes. A section of the mesh is shown in Figure 2. As can be seen, the mesh is finest at the shear layers of the mean flow. The velocity field as well as the vortcity field of the resulting mean flow is shown in Figure 3 and Figure 4, respectively.
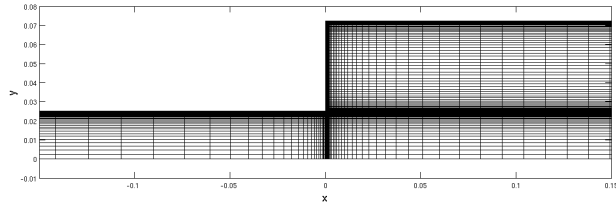

Figure 2: Overview of the mean flow mesh in the viscinity of the area expansion. Every second node in the vertical direction, and every fouth node in the horizontal direction is shown.
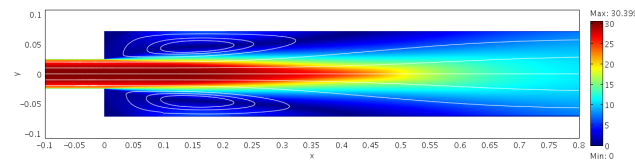

Figure 3: Magnitude of the velocity field with streamlines of the mean flow, $[m/s]$.
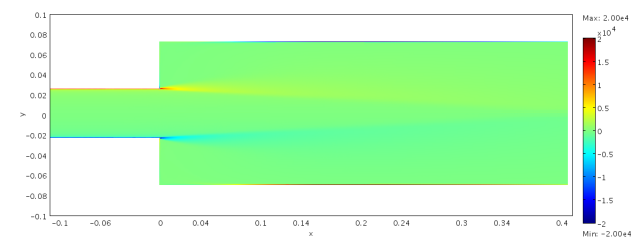

Figure 4: Vorticity field of the mean flow, $[s^{-1}]$.

SOUND FIELD

Once the mean flow is known, the perturbation field is calculated from the equation system (4-6). The frequencies were chosen to correspond to those measured in the experiments of [10], and is within the frequency range 200 Hz < f < 3000 Hz

The simulations were carried out in COMSOL Multiphysics, on the mesh shown in Figure 5, yielding a system of 864510 degrees of freedom when using third order lagrangian interpolation shape functions. This mesh will resolve the acoustic waves well enough, with just over 20 elements per acoustical wavelength at the coarsest point at the highest frequency. Calculations on this mesh resulted in an approximate solution time of five minutes per frequency on a standard PC.

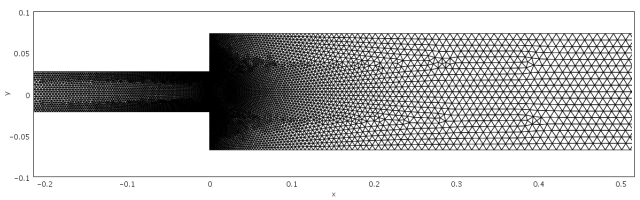In Figures 6 and 7, examples of density perturbation fields

Figure 5: Overview of the computational mesh for the acoustical calculations, shown in the viscinity of the area expansion.

and acoustic-induced vorticity fields are shown for two the different frequencies f = 500 Hz and f = 2500 Hz. An acoustic plane wave is inserted into the system from the left side and is scattered at the area expansion. The linearized Navier-Stokes eqs. support both irrotational and solenoidal parts, i.e. both acoustic waves as well as vorticity contributions are present in the perturbation field. The vortices can be seen to grow in the shear layer of the mean flow, and are convected along the stream lines of the mean flow.

Figures 8 and 9 shows the acoustic-induced vorticity. When the acoustic waves are scattered at the area expansion edges, some of the energy in the acoustic waves will be transformed into vorticial energy. This energy transfer will thus act as a dissipative effect on the acoustic waves, which leads to energy losses from the sound waves.
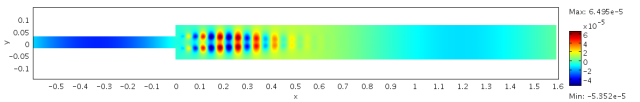

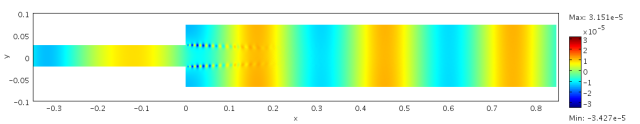Figure 6: Overview of the perturbed density field at 500 Hz.

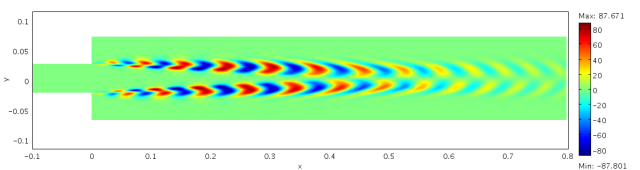Figure 7: Overview of the perturbed density field at 2500 Hz.

Figure 8: Overview of the perturbed acoustics-induced vorticity field at 500 Hz.

It can be seen that the vorticial intensity is higher in Figure 9 than in Figure 8, i.e. the vorticial intensity increase with frequency. If this is due to energy transfer from the acoustic waves or due to amplification effects from the mean flow needs to be investigated.

FREQUENCY SCALING

Due to the 2D approximation of the geometry, acoustical events occur at different frequencies compared to the full 3D cylindrical geometry. According to the theory of [8, 11], it is possible to introduce a frequency scaling to enable a compari-
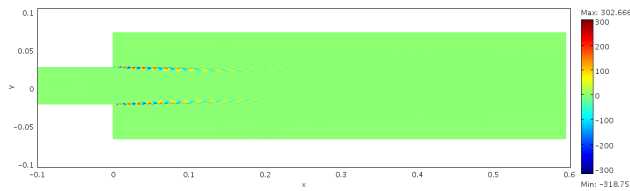
Figure 9: Overview of the perturbed acoustics-induced vorticity field at 2500 Hz.

Figure 10: Principles of the acoustic 2-port.

son of acoustic propagation in 2D and 3D, the so-called non-dimensional Helmholtz number He^*. The non-dimensional Helmholtz number is defined as the Helmholtz number divided by the Helmholtz number of the cut-on frequency of the first higher-order propagating duct mode, i.e.

$$He^* = He/He_{cut-on}. \tag{7}$$

With this frequency scaling, the relation between the 2D frequencies and the corresponding cylindrical 3D frequencies can be identified as

$$f_{2D} = \frac{r}{h}\frac{\pi}{\kappa_0}f_{cyl}, \tag{8}$$

where r is the radius of the downstream duct in cylindrical 3D, h is the height of the downstream duct in 2D, and κ_0 is the fist zero to the zeroth order Bessel function.

ACOUSTICAL 2-PORTS

To quantify the low frequency acoustical behavior of in-duct components, a so-called N-port formalism is often convenient [12]. Here N is the number of ducts connected to the component. In the case of area expansions and other geometry discontinuities, the component is connected to one inflow duct and one outflow duct, and can thus be formulated as an acoustic 2-port. The methodology is valid in the plane wave region, i.e. below the cut-on frequency of the first higher order propagating duct mode.

Several formalisms exist, such as the Transfer matrix and the Mobility matrix formalisms. The most general formulation is the Scattering matrix approach [13], which for the scattering of a 2-port system can be written as

$$\begin{pmatrix} \hat{\rho}_{1-} \\ \hat{\rho}_{2-} \end{pmatrix} = \underbrace{\begin{pmatrix} R^- & T^- \\ T^+ & R^+ \end{pmatrix}}_{S} \begin{pmatrix} \hat{\rho}_{1+} \\ \hat{\rho}_{2+} \end{pmatrix} \tag{9}$$

where the waves are defined as in Figure 10. The Scattering matrix S represents how incoming acoustic waves are transmitted and reflected at the area expansion. This is called the passive part, since sound generation processes are not included. In the general case, all quantities are complex functions of frequency.

PLANE WAVE DECOMPOSITION

To obtain the up- and downstream propagating waves needed in Eq. (9) we apply a plane wave decomposition to the simulated solution. We assume that the acoustic field quantities can be written as a sum of up- and downstream propagating plane waves, as

$$\hat{\rho} = \hat{\rho}_+ + \hat{\rho}_-, \quad \hat{u} = \hat{u}_+ + \hat{u}_- \tag{10}$$
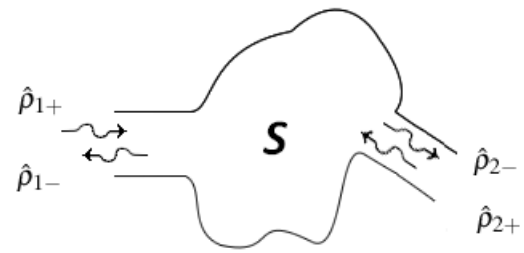
In a plane wave, the relation $\hat{\rho} = \pm \rho_0/c_0\,\hat{u}$ is valid, and thus, the wave decomposition can be written as

$$\hat{\rho}_+(x) = \frac{1}{2}\left(\hat{\rho}_{mean} + \frac{\rho_0}{c_0}\hat{u}\right) \tag{11a}$$

$$\hat{\rho}_-(x) = \frac{1}{2}\left(\hat{\rho}_{mean} - \frac{\rho_0}{c_0}\hat{u}\right) \tag{11b}$$

where *mean* is an averaging of the quantities over a duct cross section with height H, i.e. for a $2D$ case as:

$$\hat{\rho}_{mean}(x) = \frac{1}{H}\int\limits_0^H \hat{\rho}(x,y)\,dy \tag{12}$$

and correspondingly for the velocity perturbation.

RESULTS

With the acoustic wave amplitudes from the decompositions Eq. (11) inserted into the 2-port formalism, the scattering matrix Eq. (9) can be calculated.

The magnitude and phase of the scattering matrix elements are shown in Figures 11-12, respectively, along with measurements. As can be seen, the simulation results are in good agreement with the experimental results.

If the assumption made in the derivations of the methodology was to be found too restrictive, it would still be straight forward to extend the methodology. A cylindrical axisymmetric formulation could be achieved by altering the derivatives, and anisentropy by including the energy equation into the system.

If the equations (4-6) are rewritten on cylindrical form, the difference to the 2D results can be investigated. If the isentropy assumption is shown to be invalid, it is only needed to include a linearized form of the energy equation. This will however increase the size of the computations and result in more time-consuming calculations.

CONCLUSIONS

A methodology has been developed to efficiently simulate acoustic wave propagation in duct systems with arbitrary, but two-dimensional, geometries and arbitrary flows present. The methodology is based on a frequency domain formulation of the linearized Navier-Stokes equation with isentropic relations between perturbed pressure and density, to disconnect the energy equation from the linearized system of equations. The methodology was validated to measurements of the case of an area expansion with a 0.08 Mach number mean flow, with good results.
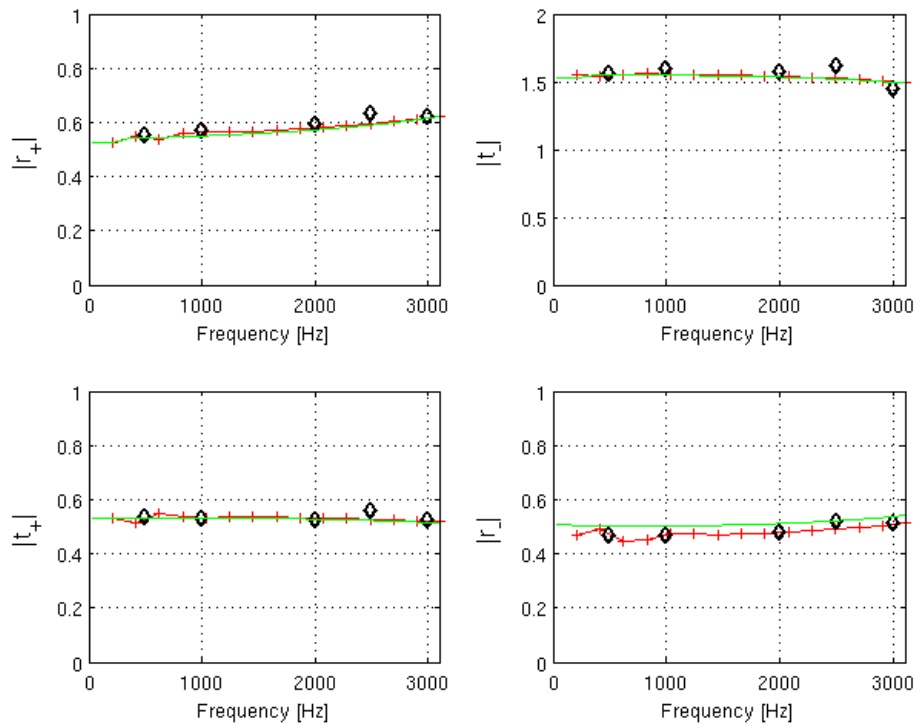
Figure 11: Magnutudes of the scattering matrix elements at an in-duct area expansion of 0.346 area ratio and Mach number $M = 0.08$ flow. Green solid line: analytical solution [8, 11], red line with + marker: simulations, black diamond markers: experimental results [10].

Figure 12: Phase normalized by π of the scattering matrix elements at an in-duct area expansion of 0.346 area ratio and Mach number $M = 0.08$ flow. Green solid line: analytical solution [8, 11], red line with + marker: simulations, black diamond markers: experimental results [10].
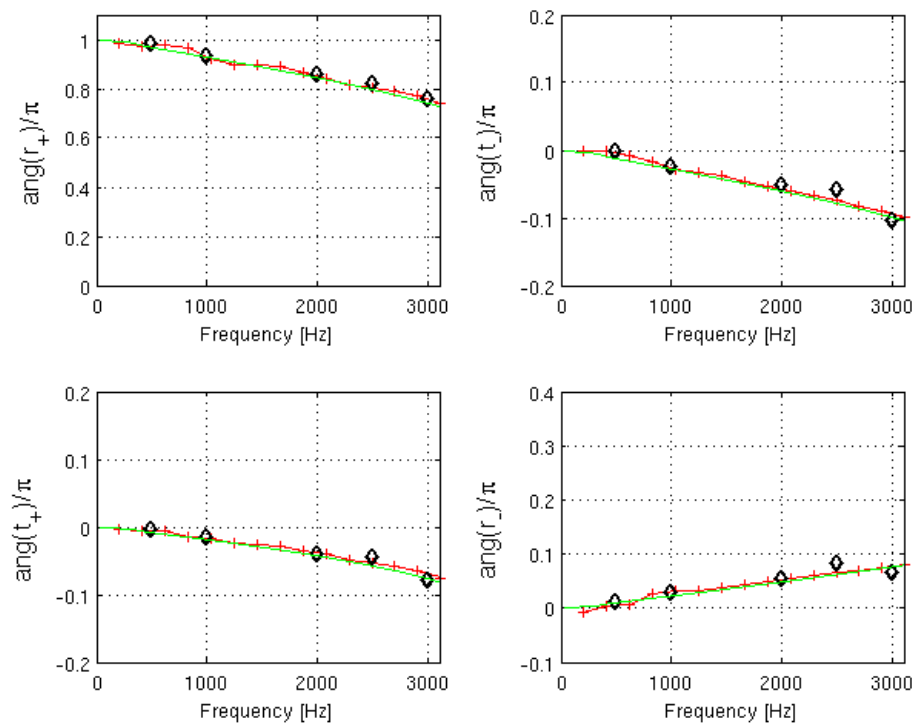
Future work will focus on expanding the methodology to also include non-isentropic relations, and cylindrical and 3D geometries.

REFERENCES

[1] Y. Özyörük, E. Dizemeny, S. Kayay, and A. Aktürkz (2007). "A Frequency Domain Linearized Euler Solver for Turbomachinery Noise Propagation and Radiation". *13th AIAA/CEAS Aeroacoustics conference*, Rome, Italy.

[2] D. Casalino, and M. Genito (2007). "Solution of Linearized Lilley's Equation in the Frequency Domain for Turbofan Aft Noise Prediction". *13th AIAA/CEAS Aeroacoustics conference*, Rome, Italy.

[3] P. P. Rao, and P. J. Morris (2006). "Use of Finite Element Methods in Frequency Domain Aeroacoustics". *AIAA Journal*, Vol. 44, No. 7.

[4] X. Gloerfelt, and P. Lafon (2008). "Direct computation of the noise induced by a turbulent flow through a diaphragm in a duct at low Mach number". *Computers & Fluids*, Vol. 37.

[5] R. Arina, R. Malvano, A. Piccato, and P. G. Spazzini (2007). "Numerical and Experimental Analysis of Sound Generated by an Orifice". *13th AIAA/CEAS Aeroacoustics Conference*, Rome, Italy.

[6] S. Föller, R. Kaess, and W. Polifke (2008). "Reconstruction of Acoustic Transfer Matrices from Large-Eddy-Simulations of Compressible Turbulent Flows". *14th AIAA/CEAS Aeroacoustics conference*, Vancouver, Canada.

[7] D. S. Henningson, M. Berggren (2005). "Fluid Dynamics: Theory and Computation". KTH.

[8] S. Boij, and B. Nilsson (2003). "Reflection of Sound at Area Expansions in a Flow Duct". *Journal of Sound and Vibration*, Vol. 260, No. 3, pp. 477-498.

[9] S. Temkin (2001). "Elements of Acoustics". *Acoustical Society of America*.

[10] D. Ronneberger (1987). "Theoretische und experimentelle Untersuchung der Schallausbreitung durch Querschnittssprünge und Lochplatten in Strömungskanälen". DFG-Abschlussbericht, Drittes Physikalisches Institut der Universität Göttingen.

[11] S. Boij, and B. Nilsson (2006). "Scattering and absorption of sound at flow duct expansions". *Journal of Sound and Vibration*, Vol. 289, pp. 577-594.

[12] H. Bodén, and M. Åbom (1995). "Modeling of fluid machines as sources of sound in duct and pipe systems". *Acta Acustica*, Vol. 3.

[13] M. Åbom (1991). "Measurement of the Scattering-Matrix of Acoustical Two-Ports". *Mechanical Systems and Signal Processing*, Vol. 5, No. 1, , pp. 89-104.